

Controlled release of enhanced cross-hybrid IgGA Fc PD-L1 inhibitors using oncolytic adenoviruses

Firas Hamdan,^{1,2,3,8} Michaela Feodoroff,^{1,2,3,4,5,8} Salvatore Russo,^{1,2,3} Manlio Fucciello,^{1,2,3} Sara Feola,^{1,2,3} Jacopo Chiaro,^{1,2,3} Gabriella Antignani,^{1,2,3} Francesca Greco,¹ Jeanette Leusen,⁶ Erkki Ylösmäki,^{1,2,3} Mikaela Grönholm,^{1,2,3,5} and Vincenzo Cerullo^{1,2,3,5,7}

¹Laboratory of Immunovirotherapy, Drug Research Program, Faculty of Pharmacy, University of Helsinki, Helsinki, Finland; ²Translational Immunology Research Program (TRIMM), University of Helsinki, Helsinki, Finland; ³Drug Delivery, Drug Research Program, Division of Pharmaceutical Biosciences, Faculty of Pharmacy, University of Helsinki, Helsinki, Finland; ⁴Institute for Molecular Medicine Finland (FIMM), Helsinki Institute of Life Science (HiLIFE), University of Helsinki, Helsinki, Finland; ⁵iCAN Digital Precision Cancer Medicine Flagship, University of Helsinki, Helsinki, Finland; ⁶Center for Translational Immunology, University Medical Center Utrecht, Utrecht, the Netherlands; ⁷Department of Molecular Medicine and Medical Biotechnology and CEINGE, Naples University Federico II, Naples, Italy

Immune checkpoint inhibitors have clinical success in prolonging the life of many cancer patients. However, only a minority of patients benefit from such therapy, calling for further improvements. Currently, most PD-L1 checkpoint inhibitors in the clinic do not elicit Fc effector mechanisms that would substantially increase their efficacy. To gain potency and circumvent off-target effects, we previously designed an oncolytic adenovirus (Ad-Cab) expressing an Fc fusion peptide against PD-L1 on a cross-hybrid immunoglobulin GA (IgGA) Fc. Ad-Cab elicited antibody effector mechanisms of IgG1 and IgA, which led to higher tumor killing compared with each isotype alone and with clinically approved PD-L1 checkpoint inhibitors. In this study, we further improved the therapy to increase the IgG1 Fc effector mechanisms of the IgGA Fc fusion peptide (Ad-Cab FT) by adding four somatic mutations that increase natural killer (NK) cell activation. Ad-Cab FT was shown to work better at lower concentrations compared with Ad-Cab *in vitro* and *in vivo* and to have better tumor- and myeloid-derived suppressor cell killing, likely because of higher NK cell activation. Additionally, the biodistribution of the Fc fusion peptide demonstrated targeted release in the tumor microenvironment with minimal or no leakage to the peripheral blood and organs in mice. These data demonstrate effective and safe use of Ad-Cab FT, bidding for further clinical investigation.

INTRODUCTION

Our immune system has a significant role in maintaining the integrity of our health. Besides its role in protecting against pathogens, it is also crucial in cancer prevention and defense. Research has indicated that immunocompromised individuals have an increased risk for developing certain cancers¹ and that mouse models with defective T cells and natural killer (NK) cells bear higher susceptibility for the disease.² Moreover, the tumor microenvironment in patients with cancer has been shown to be immunosuppressive, with tumor cells able to

develop multiple immune evasion strategies.³ Therefore, a major target in drug development for the treatment of cancer has been to boost the immune system.

An integral inhibitory pathway, the checkpoint pathway, exists within our body to modulate activation of the immune system. These checkpoints prevent the immune response from overactivation, with potential consequences being autoimmune and autoinflammatory diseases and collateral immune-mediated tissue damage. One strategy tumor cells exhibit to evade an immune response is to overexpress the negative checkpoint regulator PD-L1.^{4,5} PD-L1 is a PD-1 ligand that, upon interaction, leads to T cell exhaustion and tumor evasion. Clinical trials with PD-L1 inhibitors have demonstrated enhanced overall survival outcomes with melanoma, non-small cell lung cancer, renal cell carcinoma, and bladder cancer.⁵ However, a substantial group of patients, 66%, do not respond to such therapy, and some responders develop acquired resistance during the course of treatment.⁶ Hence, a crucial improvement in PD-L1 checkpoint inhibitors is required.

Currently, the majority of the PD-L1 inhibitors in the clinic are monoclonal antibodies (of the immunoglobulin G [IgG] isotype) that mainly act as antagonizing agents. Their pertinent effector mechanisms, such as complement-dependent cytotoxicity (CDC) or antibody-dependent cell cytotoxicity (ADCC)/antibody-dependent cell phagocytosis (ADCP), are limited or abrogated. The subsequent limitation in Fc effector mechanisms is mostly due to safety issues because PD-L1 expression is ubiquitous and can lead to killing of healthy cells. However, such effector mechanisms of many antibodies

Received 31 August 2022; accepted 31 January 2023;
<https://doi.org/10.1016/j.omto.2023.01.006>.

*These authors contributed equally

Correspondence: Vincenzo Cerullo, Laboratory of Immunovirotherapy, Drug Research Program, Faculty of Pharmacy, University of Helsinki, Helsinki, Finland.
E-mail: vincenzo.cerullo@helsinki.fi



are required for full tumor clearance. Moreover, addition of Fc effector mechanisms has been shown to increase efficacy with PD-L1 antibodies.^{7,8} This has also been shown with the approval of avelumab, which is the only IgG1 PD-L1 checkpoint inhibitor with Fc effector mechanisms in the clinic.

We previously developed a novel PD-L1 checkpoint inhibitor consisting of a PD-1 ectodomain connected to an IgGA cross-hybrid Fc, comprising regions of an IgG1 and IgA (termed Ad-Cab).⁹ All therapeutic anti-cancer antibodies in the clinic are of the IgG isotype, which is excellent in activating the complement system and NK cells. However, they fail to activate the most abundant leukocyte population, neutrophils, because of the expression pattern of Fc gamma receptors (Fc- γ). Although neutrophils express the activating receptor Fc- γ RIIA (CD32A), they have far more abundant expression of the non-signaling Fc- γ RIIB (CD16B)¹⁰ and some expression of inhibitory Fc- γ IIB (CD32B).¹¹ Contrary to IgG antibodies, IgA antibodies are able to exploit neutrophils because of expression of the activating Fc- α (CD89) receptor.^{10,12,13} However, they cannot activate the complement system (because of a lack of a C1q binding site) or NK cells (which do not express Fc- α). Therefore, the IgGA cross-hybrid Fc is able to generate effector functions of IgG1 and IgA, which leads to enhanced tumor killing and a decrease in immune effector population exhaustion.^{9,14}

Here, to further improve such therapy, we added certain point mutations in the IgG1 region of the IgGA Fc to increase NK cell activation (called Ad-Cab FT). Moreover, to circumvent toxicity issues, we cloned such a construct into an oncolytic adenovirus genome. Oncolytic adenoviruses have been shown to be ideal gene therapy vehicles because of their selective tropism and replication toward tumor cells while leaving healthy cells unharmed.^{15,16} This allows local and controlled release of our enhanced PD-L1 Fc fusion inhibitor in the tumor bed.

In this study, we demonstrated that the oncolytic adenoviruses were able to release substantial amounts of the Fc fusion peptides when infecting tumor cells. Our improved Ad-Cab FT was more potent in NK cell activation at lower concentrations compared with Ad-Cab but had a similar potency with activating the complement system and neutrophils. This also translated to higher potency with Ad-Cab FT when all effector components were added, mimicking physiological parameters. Ad-Cab FT also showed a good safety profile *in vivo* with humanized mouse models; mice did not lose weight, and release of the Fc fusion peptide was limited to the tumor with no leakage to the peripheral blood. Interestingly, other than superior tumor control, Ad-Cab FT was also able to remodel the suppressive microenvironment by reducing the presence of myeloid-derived suppressor cells (MDSCs).

RESULTS

Cab FT activates higher ADCC with peripheral blood mononuclear cells (PBMCs) at lower concentrations than Cab

Previously, we designed a novel Fc fusion peptide (Cab) consisting of a PD-1 ectodomain (binding to PD-L1) connected to a cross-hybrid

IgGA Fc via a GGGS linker. This Fc fusion peptide was able to display effector mechanisms of IgG1 and IgA, which increased tumor killing compared with clinically approved PD-L1 antibodies or IgG1 or IgA backbones alone. To further improve Cab, four point mutations (H268F/S324T/S239D/I332E) were added to the IgG1 portion of the cross-hybrid IgGA Fc (Cab FT) to increase activation of NK cells.¹⁷ We performed ADCC experiments with isolated PBMCs using different concentrations (20–0.15625 μ g/mL) of Cab and Cab FT. These experiments were performed with two murine (B16F10 and B16K1) and two human cell lines (A549 and MDA-MB-439) because the PD-1 ectodomain is able to bind to murine and human PD-L1. Moreover, we have previously tested the expression of PD-L1 and correlated the expression to specific lysis.⁹ With all cell lines, a clear trend can be observed in which Cab FT was more potent at lower concentrations (between 2.5–0.3125 μ g/mL) compared with Cab (Figure 1A). However, at high concentrations of 5–20 μ g/mL, Cab and Cab FT had similar efficiency in tumor killing (Figure 1A).

We then repeated the experiments using polymorphonuclear leukocytes (PMNs) as the effector population. No difference in killing was observed between Cab and Cab FT because IgG1 sub-optimally activates neutrophils (Figure 1B). No increase in tumor killing was observed when serum was added, even though the point mutations in Cab FT have been shown to increase C1q binding¹⁷ (Figure S1).

After seeing increased NK cell activation with Cab FT, we wanted to see whether we could observe such an effect under more physiological conditions where PBMCs and PMNs would be present. Similar to previous data, Cab FT was again superior to Cab at lower concentrations, further emphasizing the added gain in tumor killing (Figure 1C). Overall, the data demonstrate that the point mutations in Cab FT increase ADCC killing with PBMCs at lower concentrations.

Cab and Cab FT do not induce leukocyte killing and block the PD-L1/PD-1 axis

PD-L1 expression is not limited to tumor cells but can also be expressed by many immune cells, such as macrophages, dendritic cells (DCs), and monocytes. However, expression of PD-L1 has been documented to be lower compared with tumor cells. This is to our advantage because the copy number of a target epitope on the cell membrane is an essential requirement for antibody effector mechanisms to be activated. Hence, despite expression of PD-L1 on immune cells, Cab and Cab FT could not induce killing of such cell populations. To test that Cab and Cab FT do not harm crucial immune cells, we performed a whole-blood assay where unmanipulated blood from three different donors was incubated with 20 μ g/mL of both Cab and Cab FT. In the presence of all effector populations, we analyzed whether a decrease in cell percentage or absolute number was observed with T cells, NK cells, DCs, monocytes, and neutrophils (Figure 2A). No significant differences in percentages (Figure 2B) or absolute numbers (Figure 2C) were observed among samples treated with Fc fusion peptides, trastuzumab (binding to Her-2 and not found on immune cells)

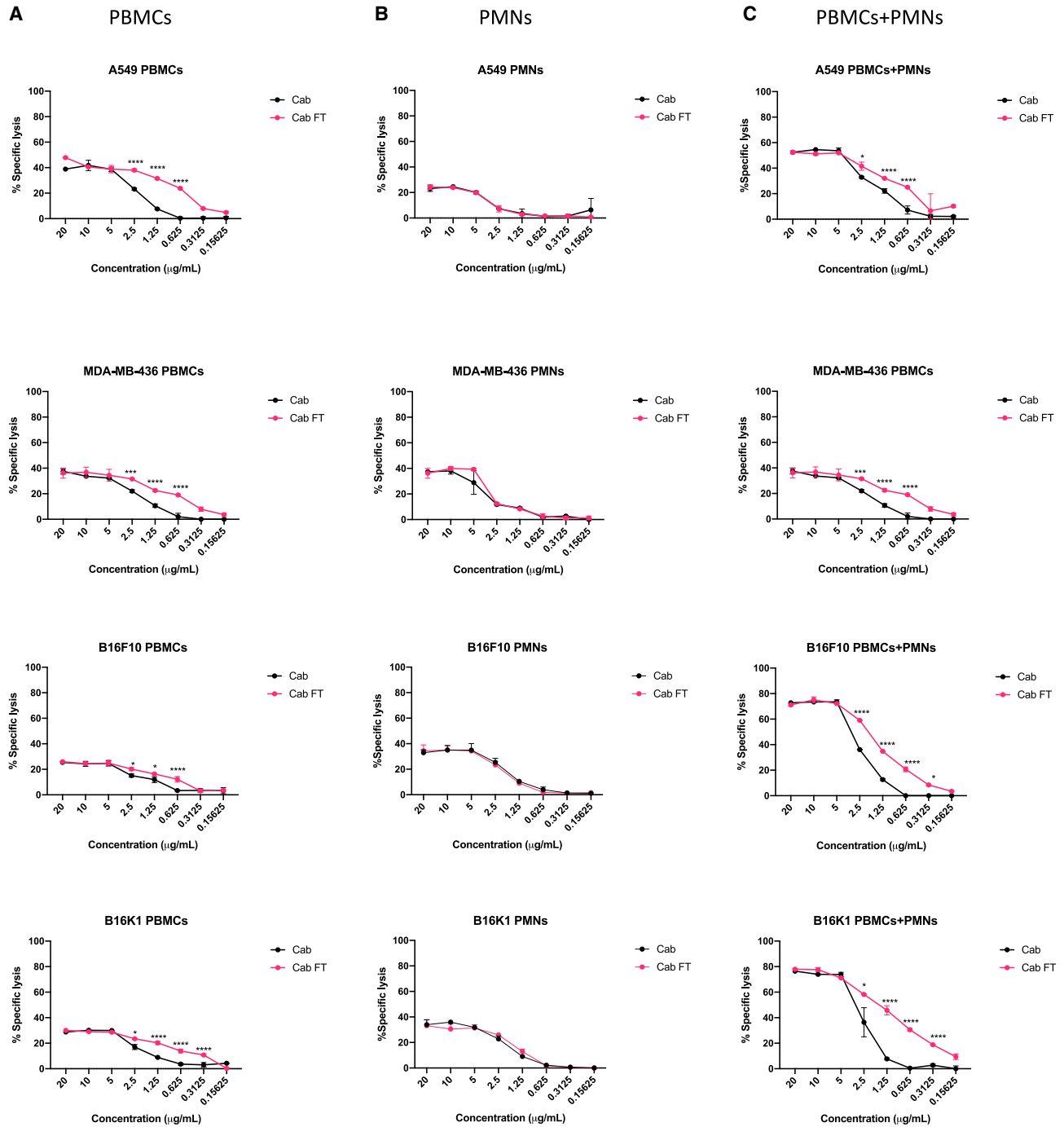


Figure 1. Cab versus Cab FT in inducing ADCC with different effector populations

(A–C) Cells were treated with different concentrations of Fc fusion peptides and had either PBMCs (A; 100:1, E:T), PMNs (B; 40:1, E:T), or PBMCs and PMNs (C) added for a 4-h incubation. Lysis was then quantified by measuring release of endogenous LDH. All $n \geq 3$, and significance levels were set at * $p < 0.05$, ** $p < 0.01$, *** $p < 0.001$, and **** $p < 0.0001$. Error bars represent SEM.

or untreated samples. This indicates that, even though Cab and Cab FT induce high tumor killing, they do not kill low-PD-L1-expressing immune cells.

Some studies have shown that increasing Fc effector functions of PD-L1 checkpoint inhibitors can lead to a higher disruption of the PD-L1/PD1 axis.¹⁸ To test whether the enhanced killing of Ad-Cab FT was

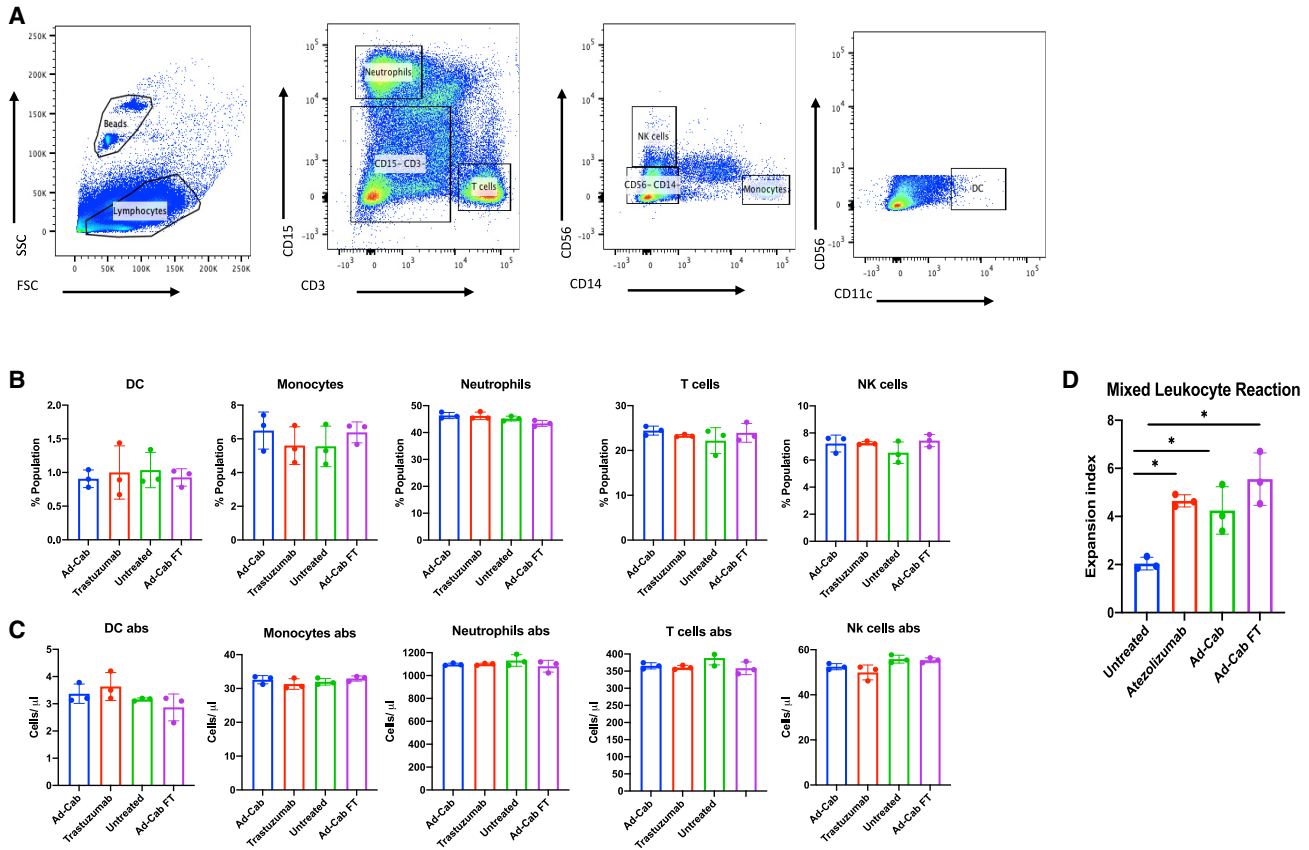


Figure 2. Whole-blood and mixed-leukocyte assay with Cab and Cab FT
 Unmanipulated blood from 3 donors was treated with 20 µg/mL of Fc fusion peptides and incubated for 24 h. (A–C) Immune populations were then gated (A) and quantified by percentage (B) and absolute number (C). DCs and CFSE-labeled PBMCs from different donors were incubated with 10 µg/mL of Fc fusion peptides or antibody for 5 days. (D) PBMCs were then collected, and CD8+ T cells had their expansion index calculated based on CFSE staining. All n ≥ 3, and significance levels were set at *p < 0.05, **p < 0.01, ***p < 0.001, and ****p < 0.0001. Error bars represent SEM.

due to the point mutations and not increased PD-L1/PD1 disruption, we performed a mixed leukocyte reaction assay. In this assay, the PD-L1/PD1 axis is analyzed by co-incubating monocyte-derived DCs from one donor with carboxyfluorescein succinimidyl ester (CFSE)-stained PBMCs from another donor. Because of the presence of PD-L1 and PD1, we expect to see very little proliferation. However, in the presence of a PD-L1 checkpoint inhibitor, an increase in the expansion should be observed. Cab and Cab FT had expansion indices very similar to each other and to the clinically approved PD-L1 checkpoint inhibitor atezolizumab (Figure 2D). Hence, Cab and Cab FT have similar levels of PD-L1/PD-1 axis inhibition.

Ad-Cab and Ad-Cab FT have similar oncolytic activity and expression levels of the Fc fusion peptide

To reduce safety concerns, Cab and Cab FT were cloned into an oncolytic adenovirus-5/3 named Ad-Cab and Ad-Cab FT, respectively. After isolating the cloned viruses, a colorimetric method for determining cell viability (3-(4,5-dimethylthiazol-2-yl)-5-(3-carboxymethoxyphenyl)-2-(4-sulphophenyl)-2H-tetrazolium [MTS] assay) was

performed to assess oncolytic fitness. In human cell lines (MDA-MB-436 and A549), clear cell lysis was observed as the multiplicity of infection (MOI) increased up to 100. Ad-Cab and Ad-Cab FT had very similar levels of cell lysis, also when compared with unarmed Ad-5/3 Δ24 (Figure 3A), which is identical to Ad-Cab viruses but lacks the Fc fusion peptide gene. This indicated that Ad-Cab and Ad-Cab FT had similar oncolytic fitness and that the gene manipulation did not affect fitness/oncolysis/functionality. As expected, no cell lysis was observed in any of the murine cell lines (B16F10, B16K1, and 4T1) (Figure 3A). This is due to the lower replication of human Ad-5 viruses in murine cells.

We then tested whether Ad-Cab and Ad-Cab FT could express and secrete the Fc fusion peptides into the supernatant. Cab and Cab FT had a His tag, allowing such quantification. When A549 cells were infected at 100 MOI, a clear secretion of Fc fusion peptide was observed. This secretion level increased until reaching day 3 post infection, when around 7 µg/mL of released peptides was detected (Figure 3B). Similar results were shown with B16K1 but with lower

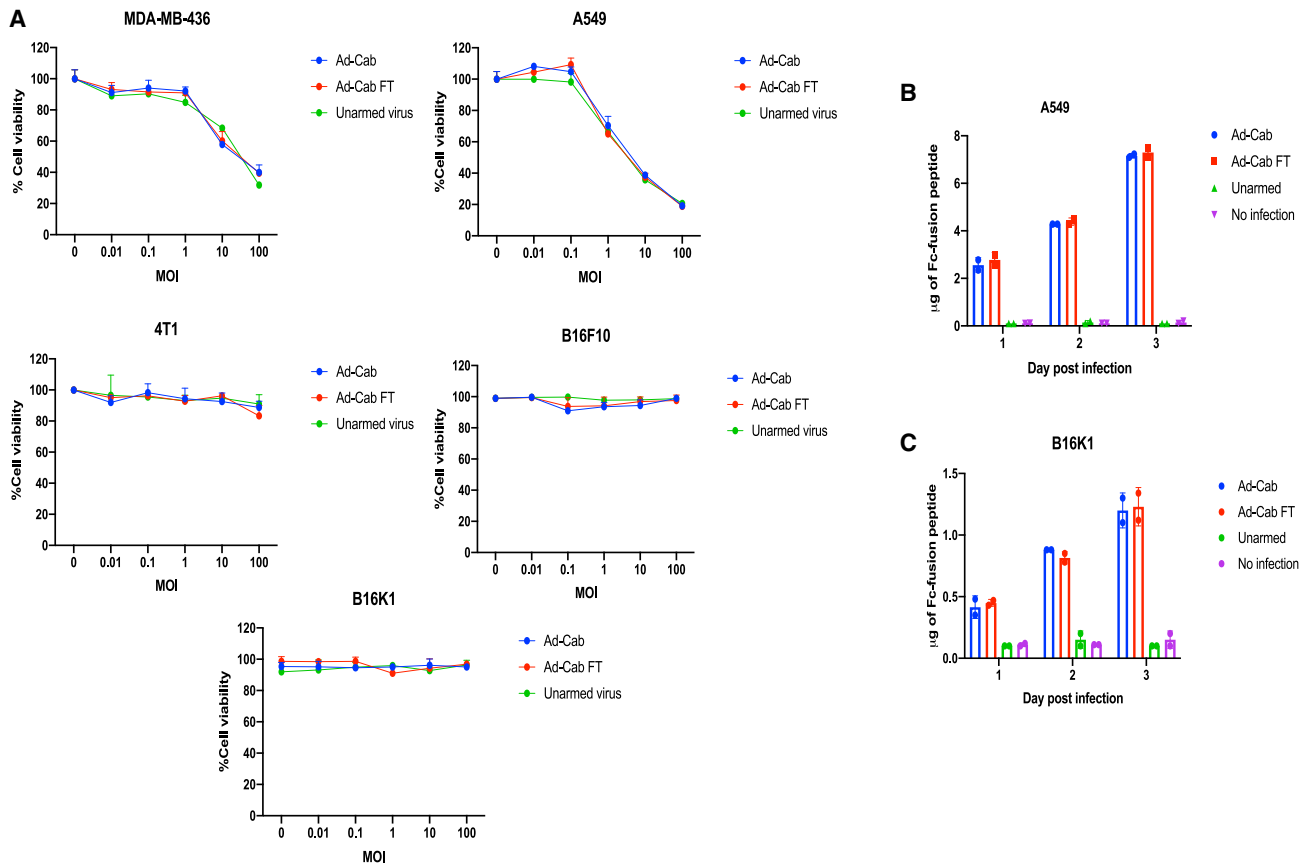


Figure 3. Oncolytic fitness and expression of Ad-Cab and Ad-Cab FT

(A–C) Different cell types were infected with the indicated MOIs of virus and incubated for 3 days. Using an MTS assay, cell viability (A) was determined. A549 (B) and B16K1 (C) cells were infected with 100 MOI of virus, and the amount of Fc fusion peptides was measured using a His tag ELISA.

amounts of secreted peptide (Figure 3C). Lower peptide levels in B16K1 are mostly due to lower adenoviral replication of Ad-5 in murine cells compared with human cells¹⁹ (Figure 3C). Together, these results indicate that Ad-Cab and Ad-Cab FT are able to express and secrete adequate levels of the Fc fusion peptide in human and murine settings.

Ad-Cab FT induces higher levels of killing at lower concentrations when PBMCs are added

To test whether the secreted Fc fusion peptides from the adenovirus were functional, we infected target cells with Ad-Cab and Ad-Cab FT and again performed ADCC assays. When human cells were infected at different MOIs ranging from 10–100, Ad-Cab FT outperformed Ad-Cab when PBMCs were added as an effector population at lower MOIs (Figure S2A). Moreover, no death was observed with Ad-5/3 Δ 24, indicating that cell lysis was due to the Fc fusion peptide and not because of viral oncolysis. With murine cells, higher MOIs were added because secretion of the Fc fusion peptide is lower compared with human cells. Similar to human cells, higher specific cell lysis could be observed with Ad-Cab FT at lower MOIs compared with

Ad-Cab. We then repeated the same experiments by adding either PMNs (Figure S2B) or complement-active serum (Figure S2C). As expected, when PMNs or serum was added, clear cell lysis was observed among Ad-Cab and Ad-Cab FT but not Ad-5/3 Δ 24. Additionally, similar specific cell lysis levels were seen with Ad-Cab and Ad-Cab FT at different MOIs.

We then performed the same experiments but with effector populations combined: PBMCs and PMNs (Figure 4). Ad-Cab FT demonstrated higher tumor cell killing levels compared with Ad-Cab at lower concentrations. Hence, Ad-Cab FT can secrete functional Cab FT and induce high tumor killing at lower MOIs when PBMCs are used as effector cells.

Ad-Cab FT induces faster killing than Ad-Cab

To further elucidate the advantages of Ad-Cab FT, we examined the kinetics of tumor killing using an impedance-based real-time quantitative analysis (XCELLigence). A549 cells were infected at 30 MOI and co-incubated with PBMCs and PMNs (Figure 5A). Cell killing was analyzed in real time, and at around 18 h, killing could be

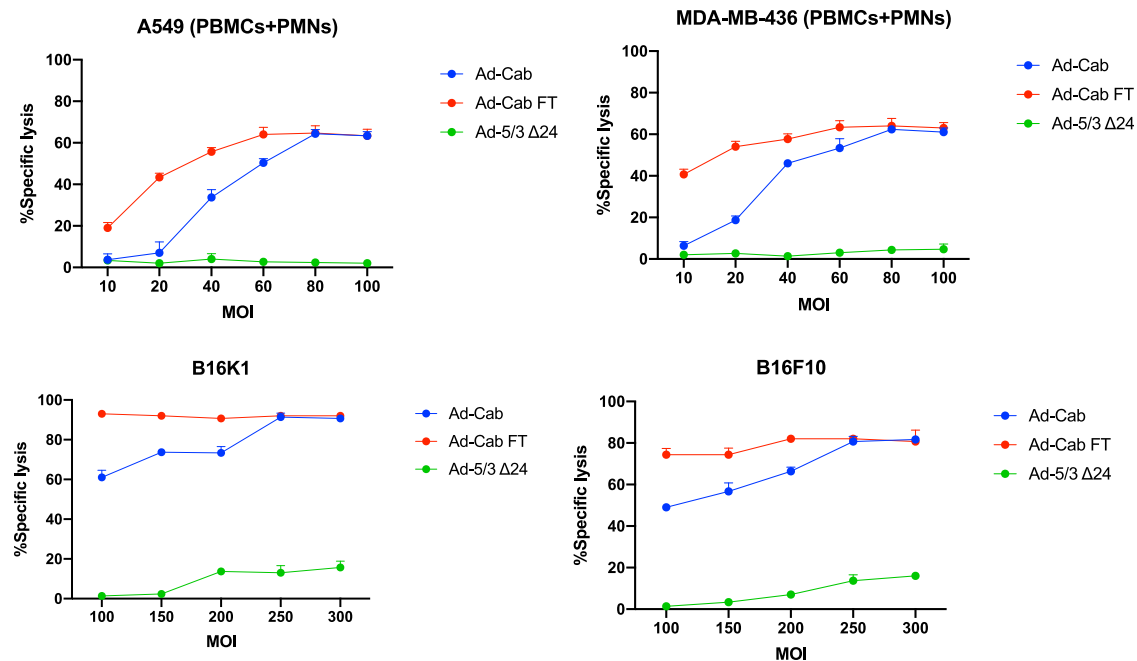


Figure 4. ADCC of Ad-Cab and Ad-Cab FT in the presence of PBMCs and PMNs

Cells were infected at various MOIs with virus and incubated for 48 h. PBMCs (100:1, E:T) and PMNs (40:1, E:T) were then added. After 4 h, lysis was quantified based on endogenous LDH release.

observed in A549 cells with Ad-Cab FT. No death was recorded at this time point with either Ad-Cab or Ad-5/3 Δ24. Cell killing for Ad-Cab and Ad-5/3 Δ24 started at around 32 and 40 h, respectively. Moreover, within 24 h, Ad-Cab FT had reached its final cell killing capacity, much earlier than the effects of viral oncolysis that were recorded with Ad-5/3 Δ24 or Ad-Cab, for which it took more than 36 h. The level of cell killing was superior with Ad-Cab FT compared with Ad-Cab, which corresponds with our previous data. In agreement with the A549 data, similar kinetics were also observed with B16K1 (Figure 5B). However, cell killing was observed later, at around 27 h for Ad-Cab FT, while for Ad-Cab, it was seen at around 42 h. These data clearly indicate that Ad-Cab FT not only kills tumor cells at a higher efficiency but also does so at a faster pace than Ad-Cab.

Ad-Cab FT controls tumor growth *in vivo* with B16K1 and 4T1

Following the *in vitro* data, we assessed the efficacy of Ad-Cab and Ad-Cab FT *in vivo* with different tumor models. For the first tumor model, we used B16K1 because of its high expression of PD-L1. Mice were sub-divided into five treatment groups receiving different treatments: PBS (mock), Ad-5/3 Δ24, Ad-Cab, Ad-Cab FT, and mPD-L1. Four injections of each treatment were given intratumorally (viruses or PBS) or intraperitoneally (antibodies), with a 2-day break between the injections (Figure 6A). Usually, 10^9 viral particles are administered per mouse for oncolytic adenovirus therapy. However, because Ad-Cab FT was shown to work at lower MOIs, each mouse was administered a one-tenth lower dose, 10^8 viral particles. As expected, Ad-Cab FT outperformed all other treatment groups

(Figures 6B and S4A). Two days after the last dose, mice were sacrificed to investigate the tumor microenvironment. Interestingly, as *in vitro*, higher NK cell activation was seen with Ad-Cab FT, explaining better tumor control than with Ad-Cab (Figure 6C). High upregulation of CD107a was observed with NK cells from the Ad-Cab FT group, which signifies a release of cytotoxic molecules such as perforins and granzymes. Upregulation of CD107a was also seen with CD8+ T cells in the Ad-Cab, Ad-Cab FT, and mPD-L1 groups because of PD1/PD-L1 inhibition (Figure 6D). Analyzing the tumor microenvironment indicates a clear increase in NK cell infiltration in Ad-Cab FT-treated groups (Figure S4B), while similar levels of CD8+ T cells (Figure S4C) and CD4+ T cells (Figure S4D) can be seen in all groups. We then tested the biodistribution of the Fc fusion peptide in the tumor and liver. In both Ad-Cab and Ad-Cab FT treated groups (Figure 6E), 1 μg/mL of Fc-fusion peptide could be observed in the tumor and undetectable levels were measured in the liver (Figure 6F). Overall, Ad-Cab FT was able to control tumor growth at lower dosages than Ad-Cab, with a safe biodistribution.

After observing the added benefit of Ad-Cab FT with B16K1, we repeated the same experiment but with a highly immunosuppressive and fast-growing tumor model, 4T1. Similar groups, schedules, and dosages were used (Figure 6G). Comparable with B16K1, Ad-Cab FT groups had the best tumor control compared with other groups (Figures 6H and S5A). Ad-Cab was also able to control tumor growth better than mPD-L1 or mock. After sacrificing the mice, we evaluated different immune cell populations. One of the main reasons why 4T1

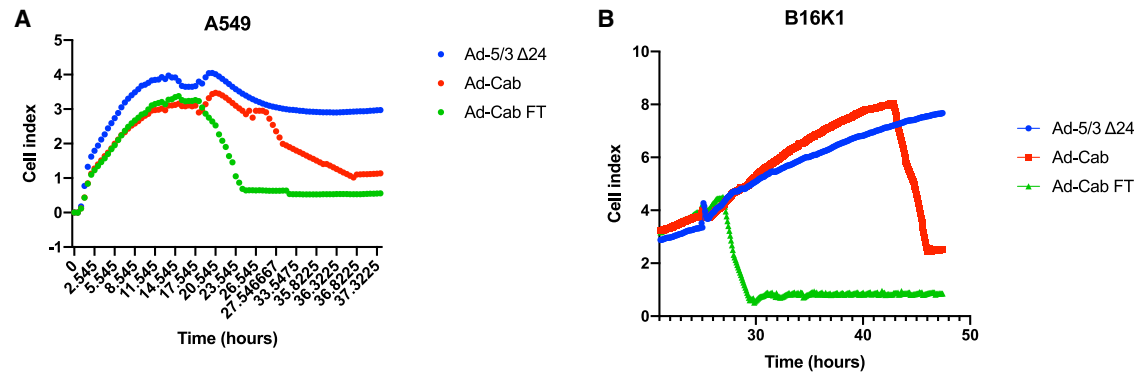


Figure 5. Real-time killing of A549 and B16K1 cells with Ad-Cab and Ad-Cab FT

(A and B) A549 (A) and B16K1 (B) cells were first seeded for 24 h. Then viruses were added at 30 MOI (A549) and 100 MOI (B16K1), along with PBMCs (100:1, E:T) and PMNs (40:1, E:T). The cell index was then measured every 30 min for the indicated times.

tumors are immunosuppressive is high infiltration of MDSCs. A decrease in MDSC granulocytic (Figure 6I) and MDSC monocytic (Figure 6J) cells can be seen in Ad-Cab FT groups, most likely because of the high expression of PD-L1. Furthermore, an increase in NK cells (Figure S5B) can be seen in Ad-Cab FT-treated groups, along with high activation (CD107a+) (Figure S5C) of such cells. Nevertheless, no changes in infiltration were seen with other immune populations, like CD8+ (Figure S5D) or CD4+ (Figure S5E) T cells, among the treated groups. Finally, a similar biodistribution was observed with around 1 µg/mL of Fc fusion peptide in the tumor microenvironment (Figure 6K) and below-detection levels in the liver (Figure 6L). In conclusion, Ad-Cab FT was able to control 4T1 tumor growth, mostly because of NK cell activation and downregulation of MDSC populations.

Ad-Cab FT is effective in controlling the A549 tumor xenograft model *in vivo*

As a final tumor model to assess efficacy, we used nonobese diabetic (NOD)/severe combined immunodeficiency (SCID) (NS)-deficient mice with a reconstituted human immune system and A549 tumor xenografts. NS mice were first implanted with A549 tumor cells and then injected with freshly isolated PBMCs from a healthy donor (Figure 7A). Before treatment, two mice injected with or without PBMCs were sacrificed. Mice injected with PBMCs could be seen to have engrafted human CD45+ cells and human CD3+ T cells (Figure 7B). Mice were then treated with PBS (mock), Ad-5/3 Δ24, Ad-Cab, or Ad-Cab FT for a total of two injections. Two injections were given instead of four, as done previously with B16K1 and 4T1 tumor models, because a higher amount of Fc fusion peptide can be obtained with the human cell line A549 compared with murine cells because of replication kinetics. As expected, mice receiving Ad-Cab FT had the best tumor control compared with any of the other groups (Figures 7C and S6). Ad-Cab did exert a therapeutic effect, but it was low and comparable with mice receiving Ad-5/3 Δ24. When examining the tumor microenvironment, the Ad-Cab and Ad-Cab FT groups had upregulation of CD107a on NK cells, indicating activation (Figure 7D). This upregulation was nevertheless higher for Ad-Cab

FT compared with Ad-Cab, which coincides with *in vitro* data. As for CD8+ T cells, similar levels of CD107a (Figure 7E) and PD1 (Figure 7F) can be seen between Ad-Cab and Ad-Cab FT. These levels were higher compared with the Ad-5/3 Δ24 group, indicating an increase in T cell activation and exhaustion. Finally, we checked the biodistribution of the Fc fusion peptides. No Fc fusion peptides were found in the blood (Figure 7G), but a high amount could be observed in the tumor (Figure 7H) and very minimal levels in the liver (Figure 7I). This indicated that most of the Fc fusion peptide can be found in the tumor microenvironment, with no leakage to the blood and liver. Thus, xenograft data further showed the effectiveness of Ad-Cab FT.

DISCUSSION

Previously, we engineered a cross-hybrid Fc fusion peptide binding to PD-L1 that consisted of an Fc region made up of an IgA1- and IgG1-constant heavy domain.⁹ The inclusion of IgA1 and IgG1 supplemented the Fc fusion peptide with Fc effector mechanisms of both isotypes, resulting in higher tumor killing *in vitro*, *in vivo*, and *ex vivo*. To further improve this therapy, we supplemented the IgG1 region with four point mutations shown previously to increase NK cell killing¹⁷ (Ad-Cab FT). Ad-Cab FT was shown to activate higher NK cell tumor killing than Ad-Cab and to result in better *in vivo* tumor control with various tumor models when lower amounts were administered.

The attribute of efficacy in antibody therapy for cancer has been the ability to elicit Fc effector mechanisms.²⁰ Checkpoint inhibitors (atezolizumab and durvalumab) in the clinic have a reduced ability to elicit such mechanisms because of the antibody isotype or single-point amino acid mutations. However, *in vitro* and *in vivo* data have shown that cancer therapeutic antibodies require Fc effector mechanisms to be effective.⁸ This does not seem to apply to all checkpoint inhibitors and primarily depends on the checkpoint receptor. For example, when CTLA-4²¹ and PD-L1^{7,8} checkpoint inhibitors had a competent Fc able to elicit effector mechanisms, it enhanced anti-tumor efficacy *in vivo*. However, for PD-1 checkpoint inhibitors,

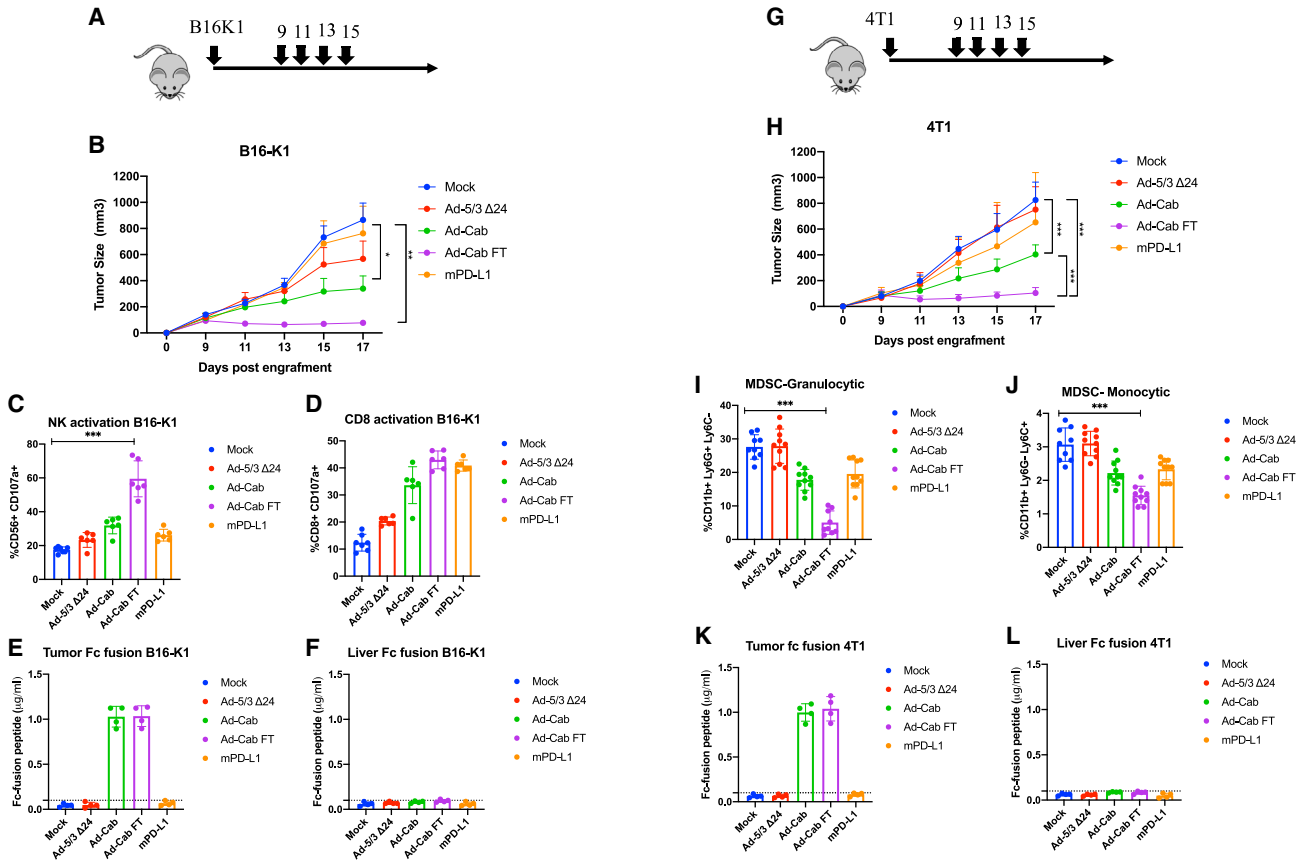


Figure 6. In vivo efficacy of Ad-Cab and Ad-Cab FT

(A) Schematic of B16K1 tumor implantation and the treatment schedule. Mice were implanted with 500,000 cells in the right flank and then treated either with PBS (mock), Ad-5/3 Δ 24, Ad-Cab, Ad-Cab FT, or mPD-L1. (B) Tumor growth was then recorded. (C and D) After mice were sacrificed, NK cell activation (C) and T cell activation (D) were measured with flow cytometry. (E and F) Biodistribution of the Fc fusion peptide was then checked in the tumor (E) and liver (F). (G) Schematic of the treatment schedule for mice implanted with 300,000 4T1 cells. The same treatment groups as for the 4T1 tumor model were used with B16K1 mice. (H) Tumor growth was recorded for 17 days. (I and J) After mice were sacrificed, suppressive immune cell populations, MDSC-granulocytic (I) and MDSC-monocytic (J), were analyzed with flow cytometry. (K and L) The biodistribution of Fc fusion peptides was analyzed in the tumor (K) and liver (L). All $n \geq 3$, and significance levels were set at * $p < 0.05$, ** $p < 0.01$, *** $p < 0.001$, and **** $p < 0.0001$. Error bars represent SEM.

having a competent Fc had negative effects on efficacy because of a reduction of effector CD8+ T cells.⁸ The contrasting effects can be attributed to expression patterns of immune checkpoints that differ among immune cells.

Coinciding with previous results, we show that incorporating effector mechanisms into PD-L1 immune checkpoint inhibitors (ICIs) increases efficacy and enhances tumor killing. Moreover, in syngeneic mouse models, PD-L1 ICIs with ADCC capabilities did not reduce or deplete neutrophils, DCs, NK cells, T cells, or B cells despite expressing PD-L1.⁸ Nevertheless, the enhanced efficacy was due to depletion of two major immunosuppressive populations: MDSCs and F4/80+ tumor-associated macrophages (TAMs). Contrary to our results, we did not see a decrease in TAMs. This can be explained by the fact that TAMs are a heterogeneous group of cells that can be polarized to either M1 or M2.²² M1 cells usually express a lower

amount of PD-L1 compared with M2, and the frequency of infiltration among these cell types can differ from that of tumor models. However, our results confirm that Fc-competent PD-L1 checkpoint inhibitors lead to a decrease in MDSC populations.

IgG antibodies can orchestrate immune cell killing of tumor cells by binding to their respective receptors, Fc- γ receptors. Six of these receptors are found in humans and can be divided into activating and inhibitory receptors. The mutations added in Ad-Cab FT selectively increase the binding of two activating Fc- γ receptors, Fc- γ IIa (CD32A) and Fc- γ IIIa (CD16A).¹⁷ NK cells only possess two Fc- γ receptors, CD16A and CD32C, which are both activating. This could potentially explain why Ad-Cab FT outperformed Ad-Cab at lower concentrations in lysing tumor cells in the presence of PBMCs. This phenomenon was not seen when PMNs were added, despite expression of CD32A on such cells. This is most likely because the

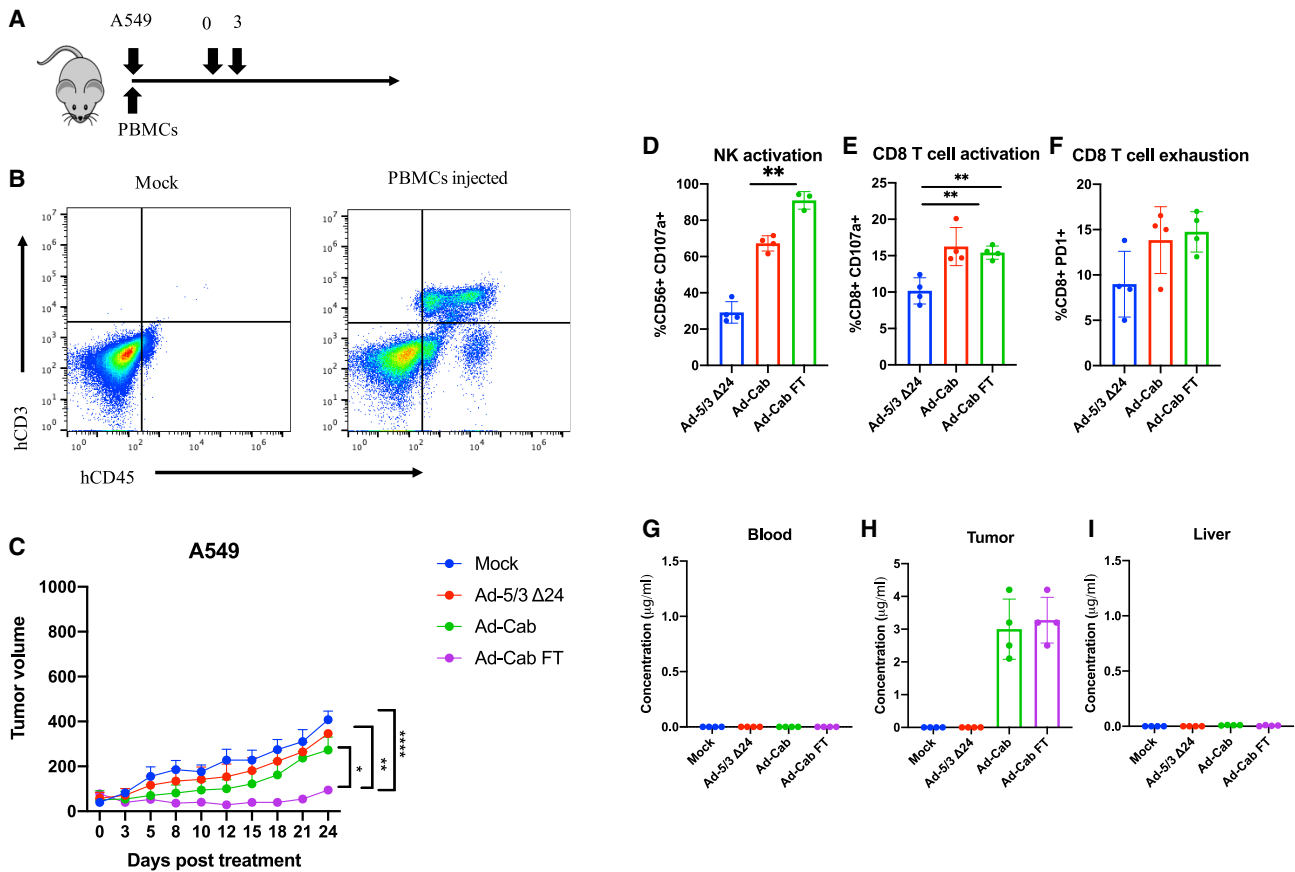


Figure 7. Efficacy of Ad-Cab and Ad-Cab FT in xenograft *in vivo* models

(A) Schematic of treatment schedules given to NS mice. Mice were first implanted in the right flank with 5×10^6 A549 cells subcutaneously and 5×10^6 PBMCs intraperitoneally. Treatment groups were divided into mice receiving Ad-5/3 Δ 24, Ad-Cab, or Ad-Cab FT. (B) Before treatment, two mice implanted with PBMCs or not were sacrificed, and human CD3⁺ and CD45⁺ cells were analyzed in the peripheral blood. (C) Tumor growth was recorded. (D–F) After mice were sacrificed, NK cell activation (D), T cell activation (E), and T cell exhaustion (F) were analyzed in the tumor microenvironment. (G–I) Biodistribution of the Fc fusion peptide was then checked in the blood (G), tumor (H), and liver (I). All $n \geq 3$, and significance levels were set at * $p < 0.05$, ** $p < 0.01$, **** $p < 0.0001$, and ***** $p < 0.00001$. Error bars represent SEM.

mutations in Ad-Cab FT also increase the affinity toward inhibitory receptor CD32B by 9.9-fold.¹⁷ Moreover, PMNs also express a higher level of CD16B, which does not possess a signaling motif but has been seen to serve as an inhibitory receptor in cancer therapy. Similarly, no increase in CDC activation was observed with Ad-Cab FT, despite the mutations being reported to increase the affinity for C1q. Induction of the classical pathway in complement activation does not solely require the Fc; the Fab regions are required, too.²³ The Fc fusion peptides lack the Fab regions, and this could explain why an increase in CDC activation was not observed.

Studies have demonstrated that the armamentarium of the immune system in the fight for cancer is finite.²³ The phenomenon of immune cell exhaustion has rendered many cancer immunotherapies ineffective in tumor clearance. Hence, activation of multiple immune effector populations seems to be a viable solution to overcome exhaustion. Along with previous studies,^{9,24} activation of multiple effector populations by simultaneously stimulating Fc- γ and Fc- α receptors has led to

higher tumor killing and less immune cell exhaustion. This study further confirms such findings as well as builds on the use of point mutations to further increase Fc effector mechanisms and tumor killing. Nevertheless, administering such potent Fc fusion peptides intravenously could be very toxic because PD-L1 is expressed all over healthy cells. Hence, to increase efficacy while maintaining the safety of PD-L1 checkpoint inhibitors, use of oncolytic viruses is favorable. In this study, we have shown that Ad-Cab and Ad-Cab FT were able to release the Fc fusion peptides and maintain them in the tumor. Very minimal or low detection levels of the Fc fusion peptides were found in the blood or liver. Usually, IgG antibodies have a half-life of 4–6 days in mice because of the presence of neonatal Fc receptors.²⁵ However, the Fc fusion peptides lack the binding domain to these neonatal Fc receptors, explaining why they were not detected in the blood. Moreover, Ad-Cab FT requires low doses to be effective, leading to low levels of the Fc fusion peptide being released. However, as mentioned, Ad-5 viruses do not replicate efficiently in murine settings, which could explain why the Fc-fusion peptide was not found outside of the tumor.

Further biodistribution studies are required, using more appropriate models, such as Syrian gold hamsters and non-human primates. These data show an encouraging safety profile of Ad-Cab and Ad-Cab FT and encourage clinical testing.

One of the main advantages of using adenoviruses as a therapeutic treatment is the feasibility of upscaling large amounts for clinical therapy. However, the purification process of adenoviruses has been an issue because the amount of adenovirus increases. For a therapeutic effect, 10^{13} viral particles of oncolytic viruses are given per patient, which causes purification to be an obstacle. In this study, we have shown that Ad-Cab FT requires a lower concentration to be administered to mice to control tumor growth. This could also translate into lower dosages of Ad-Cab used in the clinic with patient and as result ease purification issues with adenovirus production. In the future, Ad-Cab FT should undergo phase I/IIb clinical testing to investigate whether lower dosages of the virus is as effective compared to higher dosages of Ad-Cab.

One of the main limitations of Ad-Cab and Ad-Cab FT is long-term tumor control because oncolytic adenoviruses are usually administered intratumorally. For tumor types such as melanoma or other easily accessible tumors, repeated injections can be possible and can help with long-term tumor control. However, for tumors that are in deep tissues, this can pose a problem; guided surgical instruments are required, and repeated injections might be inconvenient for patients and pose a possible health risk. As for metastatic tumors, Ad-Cab or Ad-Cab FT would have very little effect because of the poor biodistribution of the Fc fusion peptides. One way to overcome this limitation is by adding a vaccine effect to the platform, such as attachment and/or genetic cloning of tumor peptides.

Conclusion

In this work, we further improved a previously designed PD-L1 Fc fusion peptide consisting of a cross-hybrid IgG_A Fc (Ad-Cab) by adding four point mutations (Ad-Cab FT), leading to an increase in IgG effector mechanisms. At low concentrations, Ad-Cab FT was shown to secrete adequate levels of the Fc fusion peptide able to induce higher tumor killing when PBMCs were added compared with Ad-Cab. Moreover, other than higher tumor killing, Ad-Cab FT was able to induce tumor cell death faster than Ad-Cab. The effectiveness of Ad-Cab FT was also seen in different *in vivo* models, displaying better tumor control and higher activation of NK cells. Other than tumor control, Ad-Cab FT was also able to downregulate MDSC populations that have been correlated with poor prognosis and tumor growth. Finally, biodistribution analysis revealed that the oncolytic adenoviruses restricted release of the toxic Fc fusion peptides to the tumor, reducing safety concerns. In conclusion, the efficacy and safety profile of Ad-Cab FT prompt further investigation for clinical use.

MATERIALS AND METHODS

Cell lines

All cell lines in this study were purchased from the American Type Culture Collection (ATCC) and cultured in appropriate medium at

37°C and 5% CO₂. Cell lines used in this study were human lung cancer A549, human triple negative breast cancer MDA-MB-436, murine triple negative breast cancer 4T1, and murine skin cancer B16K1 and B16F10. All cell lines were cultured until reaching passage 15 and routinely checked for mycoplasma infection.

Virus transgene modifications

Adenoviruses were made to be conditionally replicating, using protocols described previously.²⁶ All adenoviruses are of serotype 5 with a fiber of serotype 3 (Ad-5/3) and contain a 24-bp deletion in the E1A region. The Fc fusion peptide transgenes were produced using the GeneArt gene synthesis service (Thermo Fisher Scientific). The Fc fusion peptide genes were then added to the adenovirus genome using protocols described previously.²⁷ In short, the gp19K + 7.1k region was substituted with the Fc fusion peptides using Gibson assembly. Moreover, the Fc fusion peptides were under a cytomegalovirus (CMV) promoter.

Cell viability assays

Cell viability was assessed by plating 10,000 cells and infecting them with various MOIs (0.01–100) for 3 days. Death was then assessed by MTS according to the manufacturer's protocol (Cell Titer 96 Aqueous One Solution Cell Proliferation Assay, Promega, Nacka, Sweden). Spectrophotometric data were read using the Varioskan LUX Multimode Reader (Thermo Scientific, Carlsbad, CA, USA).

Serum collection

Ten volunteers had 40 mL of their blood taken in BD Vacutainer collection tubes (BD Bioscience), which was left to clot for 30 min at room temperature. Following clotting, blood samples were centrifuged for 5 min at 2,500 rpm. Serum was then collected and frozen at –80°C until further use.

PBMC, PMN, and monocyte collection

PBMCs and PMNs were separated and isolated from buffy coats as described previously²⁸ and cultured in Roswell Park Memorial Institute (RPMI) 1640 medium (Gibco, catalog number 21875034). From PBMCs, monocytes were further collected as described previously.¹³

Mixed leukocyte reaction

Monocytes were first differentiated into DCs by culturing in DMEM low glucose supplemented with 10% fetal bovine serum (FBS), 500 U/mL of interleukin-4 (IL-4) (PeproTech, 200-04), and 250 U/mL (Abcam, ab88382) for 7 days. After differentiation, PBMCs from a different donor were labeled with CFSE (Thermo Fisher Scientific) according to the manufacturer's protocol, cocultured at a 1:10 ratio, and treated with 1 µg/mL of either atezolizumab (InvivoGen) or Fc fusion peptide. After 5 days, supernatants were collected, and CFSE was measured in gated CD3+ CD8+ T cells by flow cytometry.

CDC assay

CDC assays were performed either with purified Fc fusion peptides or viruses. For viruses, 100,000 cells were plated and infected at the

indicated MOIs for 48 h. For Fc fusion peptides, different concentrations as indicated were added and incubated for 30 min. After incubation, 15.5% of complement-active serum was added for 4 h. Cells were then stained with 7-aminoactinomycin D (7-AAD) (eBioscience), and lysis was measured using flow cytometry.

ADCC assays

ADCC assays were performed using either purified Fc fusion peptides or viruses. Similar to the CDC assays, 15,000 cells were infected with the indicated MOIs for 48 h, while for Fc-fusion peptides, the indicated concentration was added for 30 min. After incubation, effector cells were added at a ratio of 100:1 and 40:1 (effector:target) for PBMCs and PMNs, respectively. After 4 h of incubation at 37°C, cell lysis was measured by calculating the release of endogenous lactate dehydrogenase (LDH) using a commercial kit (CyQUANT LDH Cytotoxicity Assay, catalog number C20303). Specific percent cell lysis was calculated using the following formula: (“experimental LDH release” – “effector plus target spontaneous”)/ (“target maximum” – “effector plus target spontaneous”) × 100. “Experimental LDH release” corresponds to the signal measured by the treated samples, “effector plus target spontaneous” corresponds to the release of LDH when effectors and targets are incubated, and “target maximum” corresponds to when target cells are treated with cell lysis buffer.

Whole-blood assay

Whole blood was collected from three healthy volunteers in BD Vacutainer heparin plasma tubes (BD Bioscience). Healthy volunteers were defined as volunteers with no underlying pathologies. 200 µL of unmanipulated blood was then incubated with 20 µg/mL of antibody or Fc fusion peptides for 24 h at 37°C. After 24 h, samples were treated with ammonium-chloride-potassium (ACK) buffer to lyse red blood cells and then stained with CD3, CD15, CD14, CD56, and CD11c (BioLegend) to differentiate immune populations. Counting beads were then added before performing flow cytometry to calculate absolute numbers (BioLegend, catalog number 424902).

Animal experiments

For syngeneic mouse experiments, 4- to 8-week-old BALB/c or C57BL/6 immunocompetent mice, purchased from Envigo, were injected with 300,000 4T1 or 500,000 B16K1 cells in the right flank, respectively. After 9 days, tumors were palpable, and then followed a treatment schedule of 4 treatments separated by 2 days of break between. Viruses or PBS were injected intratumorally at a final volume of 25 µL, while antibodies were administered intraperitoneally at a final volume of 100 µL. Viruses were administered at a concentration of 1×10^8 viral particles per mouse, while 100 µg of antibody was administered per mouse. Tumor size was calculated using the following formula: (long side) × (short side)²/2.

For xenograft mice models, 4- to 6-week-old immunodeficient Nod.CB17-Prkdcscid/NCrCrl mice were purchased from Charles River Laboratories. For tumor implantation, mice were injected with 5×10^6 A549 cells subcutaneously in the right flank. On the same

day, 5×10^6 PBMCs extracted from the same donor were injected intraperitoneally for engraftment. After tumors were palpable, mice were given 2 doses of virus at a concentration of 1×10^8 viral particles per mouse.

All animal experiments were approved and reviewed by the Experimental Animal Committee of the University of Helsinki and Provincial Government of Southern Finland (license ESAVI/11895/2019). Tumor growth across all experimental groups was regularly measured throughout the experiment. All injections and tumor measurements were performed under isoflurane anesthesia.

Biodistribution analysis

After animals were sacrificed, tumors, livers, and peripheral blood were collected for processing. Tumors and livers were passed through a 0.22-µm cell strainer to create a single-cell suspension. Samples were then centrifuged for 10 min at $500 \times g$ to pellet cells and collect the supernatant for further processing. For blood, samples were centrifuged for 30 min at $500 \times g$, and serum was collected. Because the Fc fusion peptides contain a C-terminal His tag, a His tag ELISA was used to determine concentrations from the supernatant and serum samples collected (Cell Biolabs, catalog number AKR-130).

Flow cytometry analysis

All flow cytometry samples were run either with the BD Accuri 6 plus (BD Bioscience) or Fortessa (BD Bioscience). Human and murine samples had two antibody panels each that were used. Panel 1 includes fluorescein isothiocyanate (FITC) anti-mouse NK1.1 (Thermo Fisher Scientific, catalog number 11-5941-85, RRID: AB_465319), phycoerythrin (PE) anti-mouse PD-1 (BioLegend, catalog number 135206, RRID: AB_1877231), PeCy7 anti-mouse CD4 (Thermo Fisher Scientific, catalog number 25-0041-82, RRID: AB_469576), PerCp/Cy5.5 anti-mouse CD107a (BioLegend, catalog number 121626, RRID: AB_2572055), and Pacific Blue anti-mouse CD3 (BioLegend, catalog number 100214, RRID: AB_493645). Panel 2 included allophycocyanin (APC) anti-mouse Ly6C (BioLegend, catalog number 128015, RRID: AB_1732087), PE anti-Ly6G (BD Biosciences, catalog number 551461, RRID: AB_394208), PerCP Cy5.5 anti-mouse CD11b (Thermo Fisher Scientific, catalog number 45-0112-82, RRID: AB_953558), BV650 anti-mouse F4/80 (BD Biosciences, catalog number 743282, RRID: AB_2741400), and PECy7 anti-mouse CD11c (Thermo Fisher Scientific, catalog number 25-0114-829, RRID: AB_469590). For humans, the first panel included FITC anti-human CD56 (BioLegend, catalog number 304604, RRID: AB_314446), PerCP anti-human CD8alpha (BioLegend, catalog number 300922, RRID: AB_1575072), PE-Cy5 anti-human CD4 (Thermo Fisher Scientific, catalog number 15-0049-42, RRID: AB_1582251), PE-Cy7 anti-human CD3 (BioLegend, catalog number 300316, RRID: AB_314052), Pacific Blue anti-human PD-1 (BioLegend, catalog number 329915, RRID: AB_1877194), and APC anti-human CD107a (BioLegend, catalog number 328620, RRID: AB_1279055). The second panel for human samples included PE-Cy7 anti-human CD3 (BioLegend, catalog number 300316, RRID: AB_314052), APC anti-human CD11c (BioLegend, catalog number

371505, RRID: AB_2616901), Pacific Blue anti-human CD15 (BioLegend, catalog number 323021, RRID: AB_2105361), and PE anti-human CD14 (BioLegend, catalog number 301805, RRID: AB_314187).

Statistical analysis

All statistical analysis were performed with GraphPad Prism 7 (GraphPad, La Jolla, CA, USA). Statistical tests used were either unpaired t test or two-way ANOVA with a post hoc test (Tukey's multiple comparisons tests). All $n \geq 3$, and significance levels were set at * $p < 0.05$, ** $p < 0.01$, *** $p < 0.001$, and **** $p < 0.0001$. Error bars represent standard error of the mean (SEM).

DATA AVAILABILITY

The authors confirm that all data supporting the manuscript findings are available in the main text and supplemental figures. Raw data of this study are available upon reasonable request from the corresponding author.

SUPPLEMENTAL INFORMATION

Supplemental information can be found online at <https://doi.org/10.1016/j.omto.2023.01.006>.

ACKNOWLEDGMENTS

F.H. thanks the Research Foundation of the University of Helsinki for funding his doctoral studies at the Faculty of Pharmacy, University of Helsinki. V.C. acknowledges the European Research Council under the Horizon 2020 framework (<https://erc.europa.eu>), ERC-consolidator grant (agreement 681219), the Jane and Aatos Erkko Foundation (project 4705796), HiLIFE Fellow (project 797011004), the Finnish Cancer Foundation (project 4706116), the Magnus Ehrnrooth Foundation (project 4706235), the Academy of Finland, and Digital Precision Cancer Medicine Flagship iCAN.

AUTHOR CONTRIBUTIONS

F.H., J.L., E.Y., and V.C. planned and conceived the experiments. F.H. and M.Fedoroff carried out most of the experiments. S.R., M.Fusciello, S.F., J.C., G.A., F.G., E.Y., and M.G. helped to carry out the experiments and interpret results. J.L. provided significant expertise. F.H. wrote the manuscript. All authors provided critical feedback and helped shape the research, analysis, and manuscript.

DECLARATION OF INTERESTS

V.C. is a co-founder and shareholder of Valo Therapeutics LTD (not related to this study).

REFERENCES

- Vajdic, C.M., and Van Leeuwen, M.T. (2009). Cancer incidence and risk factors after solid organ transplantation. *Int. J. Cancer* *125*, 1747–1754. <https://doi.org/10.1002/IJC.24439>.
- Smyth, M.J., Thia, K.Y., Street, S.E., MacGregor, D., Godfrey, D.I., and Trapani, J.A. (2000). Perforin-mediated cytotoxicity is critical for surveillance of spontaneous lymphoma. *J. Exp. Med.* *192*, 755–760. <https://doi.org/10.1084/JEM.192.5.755>.
- Vinay, D.S., Ryan, E.P., Pawelec, G., Talib, W.H., Stagg, J., Elkord, E., Lichtor, T., Decker, W.K., Whelan, R.L., Kumara, H.M.C.S., et al. (2015). Immune evasion in can-

cer: mechanistic basis and therapeutic strategies. *Semin. Cancer Biol.* *35*, S185–S198. <https://doi.org/10.1016/J.SEMCANCER.2015.03.004>.

- Ishida, Y., Agata, Y., Shibahara, K., and Honjo, T. (1992). Induced expression of PD-1, a novel member of the immunoglobulin gene superfamily, upon programmed cell death. *EMBO J.* *11*, 3887–3895. <https://doi.org/10.1002/J.1460-2075.1992.TB05481.X>.
- Chen, L., and Han, X. (2015). Anti-PD-1/PD-L1 therapy of human cancer: past, present, and future. *J. Clin. Invest.* *125*, 3384–3391. <https://doi.org/10.1172/JCI80011>.
- Jácome, A.A., Castro, A.C.G., Vasconcelos, J.P.S., Silva, M.H.C.R., Lessa, M.A.O., Moraes, E.D., Andrade, A.C., Lima, F.M.T., Farias, J.P.F., Gil, R.A., et al. (2021). Efficacy and safety associated with immune checkpoint inhibitors in unresectable hepatocellular carcinoma. *JAMA Netw. Open* *4*, e2136128. <https://doi.org/10.1001/JAMANETWORKOPEN.2021.36128>.
- Goletz, C., Lischke, T., Harnack, U., Schiele, P., Danielczyk, A., Rühmann, J., and Goletz, S. (2018). Glyco-engineered anti-human programmed death-ligand 1 antibody mediates stronger CD8 T cell activation than its normal glycosylated and non-glycosylated counterparts. *Front. Immunol.* *9*, 1614. <https://doi.org/10.3389/FIMMU.2018.01614/BIBTEX>.
- Dahan, R., Segal, E., Engelhardt, J., Selby, M., Korman, A.J., and Ravetch, J.V. (2015). FcγRs modulate the anti-tumor activity of antibodies targeting the PD-1/PD-L1 Axis. *Cancer Cell* *28*, 285–295. <https://doi.org/10.1016/J.CCELL.2015.08.004>.
- Hamdan, F., Ylösmäki, E., Chiaro, J., Giannoula, Y., Long, M., Fusciello, M., Feola, S., Martins, B., Feodoroff, M., Antignani, G., et al. (2021). Novel oncolytic adenovirus expressing enhanced cross-hybrid IgGα Fc PD-L1 inhibitor activates multiple immune effector populations leading to enhanced tumor killing in vitro, in vivo and with patient-derived tumor organoids. *J. Immunother. Cancer* *9*, e003000. <https://doi.org/10.1136/JITC.2021-003000>.
- Bournazos, S., Wang, T.T., and Ravetch, J.V. (2016). The role and function of Fcγ receptors on myeloid cells. *Microbiol. Spectr.* *4*.
- Treffers, L.W., Van Houdt, M., Bruggeman, C.W., Heineke, M.H., Zhao, X.W., Van Der Heijden, J., Nagelkerke, S.Q., Verkuijlen, P.J.J.H., Geissler, J., Lissenberg-Thunnissen, S., et al. (2018). FcγRIIb restricts antibody-dependent destruction of cancer cells by human neutrophils. *Front. Immunol.* *9*, 3124. <https://doi.org/10.3389/FIMMU.2018.03124/BIBTEX>.
- Brandsma, A.M., Bondza, S., Evers, M., Koutstaal, R., Nederend, M., Jansen, J.H.M., Rösner, T., Valerius, T., Leusen, J.H.W., and Ten Broeke, T. (2019). Potent Fc receptor signaling by IgA leads to superior killing of cancer cells by neutrophils compared to IgG. *Front. Immunol.* *10*, 704. <https://doi.org/10.3389/FIMMU.2019.00704/BIBTEX>.
- Evers, M., Ten Broeke, T., Jansen, J.H.M., Nederend, M., Hamdan, F., Reiding, K.R., Meyer, S., Moerer, P., Brinkman, I., Rösner, T., et al. (2020). Novel chimerized IgA CD20 antibodies: improving neutrophil activation against CD20-positive malignancies. *MAbs* *12*. <https://doi.org/10.1080/19420862.2020.1795505>.
- Kelton, W., Mehta, N., Charab, W., Lee, J., Lee, C.H., Kojima, T., Kang, T.H., and Georgiou, G. (2014). IgGα: a “cross-isotype” engineered human Fc antibody domain that displays both IgG-like and IgA-like effector functions. *Chem. Biol.* *21*, 1603–1609. <https://doi.org/10.1016/J.CHEMBIOL.2014.10.017>.
- Feng, Y., Roy, A., Masson, E., Chen, T.T., Humphrey, R., and Weber, J.S. (2013). Exposure–response relationships of the efficacy and safety of ipilimumab in patients with advanced melanoma. *Clin. Cancer Res.* *19*, 3977–3986. <https://doi.org/10.1158/1078-0432.CCR-12-3243>.
- Höti, N., Li, Y., Chen, C.L., Chowdhury, W.H., Johns, D.C., Xia, Q., Kabul, A., Hsieh, J.T., Berg, M., Kötner, G., et al. (2007). Androgen receptor attenuation of Ad5 replication: implications for the development of conditionally replication competent adenoviruses. *Mol. Ther.* *15*, 1495–1503. <https://doi.org/10.1038/SJ.MT.6300223>.
- Moore, G.L., Chen, H., Karki, S., and Lazar, G.A. (2010). Engineered Fc variant antibodies with enhanced ability to recruit complement and mediate effector functions. *MAbs* *2*, 181–189. <https://doi.org/10.4161/MABS.2.2.11158>.
- Sun, L., Li, C.W., Chung, E.M., Yang, R., Kim, Y.S., Park, A.H., Lai, Y.J., Yang, Y., Wang, Y.H., Liu, J., et al. (2020). Targeting glycosylated PD-1 induces potent anti-tumor immunity. *Cancer Res.* *80*, 2298–2310. <https://doi.org/10.1158/0008-5472.CAN-19-3133>.

19. Blair, G.E., Dixon, S.C., Griffiths, S.A., and Zajdel, M.E. (1989). Restricted replication of human adenovirus type 5 in mouse cell lines. *Virus. Res.* *14*, 339–346. [https://doi.org/10.1016/0168-1702\(89\)90026-9](https://doi.org/10.1016/0168-1702(89)90026-9).
20. Desjarlais, J.R., and Lazar, G.A. (2011). Modulation of antibody effector function. *Exp. Cell Res.* *317*, 1278–1285. <https://doi.org/10.1016/j.yexcr.2011.03.018>.
21. Simpson, T.R., Li, F., Montalvo-Ortiz, W., Sepulveda, M.A., Bergerhoff, K., Arce, F., Roddie, C., Henry, J.Y., Yagita, H., Wolchok, J.D., et al. (2013). Fc-dependent depletion of tumor-infiltrating regulatory T cells co-defines the efficacy of anti-CTLA-4 therapy against melanoma. *J. Exp. Med.* *210*, 1695–1710. <https://doi.org/10.1084/JEM.20130579>.
22. Wu, L., and Zhang, X.H.F. (2020). Tumor-associated neutrophils and macrophages—heterogenous but not chaotic. *Front. Immunol.* *11*, 553967. <https://doi.org/10.3389/FIMMU.2020.553967>.
23. Mortensen, S.A., Sander, B., Jensen, R.K., Pedersen, J.S., Golas, M.M., Jensenius, J.C., Hansen, A.G., Thiel, S., and Andersen, G.R. (2017). Structure and activation of C1, the complex initiating the classical pathway of the complement cascade. *Proc. Natl. Acad. Sci. USA* *114*, 986–991. <https://doi.org/10.1073/PNAS.1616998114/-/DCSUPPLEMENTAL>.
24. Brandsma, A.M., Ten Broeke, T., Nederend, M., Meulenbroek, L.A.P.M., Van Tetering, G., Meyer, S., Jansen, J.H.M., Beltrán Buitrago, M.A., Nagelkerke, S.Q., Németh, I., et al. (2015). Simultaneous targeting of FcγRs and FcαRI enhances tumor cell killing. *Cancer Immunol. Res.* *3*, 1316–1324. <https://doi.org/10.1158/2326-6066.CIR-15-0099-T>.
25. Vieira, P., and Rajewsky, K. (1988). The half-lives of serum immunoglobulins in adult mice. *Eur. J. Immunol.* *18*, 313–316. <https://doi.org/10.1002/EJL.1830180221>.
26. Kanerva, A., Zinn, K.R., Chaudhuri, T.R., Lam, J.T., Suzuki, K., Uil, T.G., Hakkarainen, T., Bauerschmitz, G.J., Wang, M., Liu, B., et al. (2003). Enhanced therapeutic efficacy for ovarian cancer with a serotype 3 receptor-targeted oncolytic adenovirus. *Mol. Ther.* *8*, 449–458. [https://doi.org/10.1016/S1525-0016\(03\)00200-4](https://doi.org/10.1016/S1525-0016(03)00200-4).
27. Hamdan, F., Martins, B., Feodoroff, M., Giannoula, Y., Feola, S., Fucsiello, M., Chiaro, J., Antignani, G., Grönholm, M., Ylösmäki, E., and Cerullo, V. (2021). GAMER-Ad: a novel and rapid method for generating recombinant adenoviruses. *Mol. Ther. Methods Clin. Dev.* *20*, 625–634. <https://doi.org/10.1016/j.omtm.2021.01.014>.
28. Cui, C., Schoenfelt, K.Q., Becker, K.M., and Becker, L. (2021). Isolation of polymorphonuclear neutrophils and monocytes from a single sample of human peripheral blood. *STAR Protoc.* *2*, 100845. <https://doi.org/10.1016/j.xpro.2021.100845>.